Journal of Adhesion Science and Technology

ISSN: 0169-4243 (Print) 1568-5616 (Online) Journal homepage: http://www.tandfonline.com/loi/tast20

Self-assembly on copper surface by using imidazole derivative for corrosion protection

P. Durainatarajan, M. Prabakaran, S. Ramesh & V. Periasamy

To cite this article: P. Durainatarajan, M. Prabakaran, S. Ramesh & V. Periasamy (2018) Self-assembly on copper surface by using imidazole derivative for corrosion protection, Journal of Adhesion Science and Technology, 32:16, 1733-1749, DOI: 10.1080/01694243.2018.1444004

To link to this article: https://doi.org/10.1080/01694243.2018.1444004

JOURNAL OF ADHESION SCIENCE AND TECHNOLOGY, 2018
VOL. 32, NO. 16, 1733–1749
https://doi.org/10.1080/01694243.2018.1444004

Self-assembly on copper surface by using imidazole derivative for corrosion protection

P. Durainatarajan[a], M. Prabakaran[b], S. Ramesh[a] and V. Periasamy[a]

[a]Department of Chemistry, The Gandhigram Rural Institute – Deemed to be University, Gandhigram, India; [b]Department of Chemistry, Gnanamani College of Technology, Namakkal, India

ABSTRACT
This paper presents the self-assembly of 1-(3-aminopropyl) imidazole (API) monolayer on the copper surface to study the inhibition effect of the API against copper corrosion in 3% NaCl solution. The optimum concentration and assembling time for the assembly of API on copper were ascertained using electrochemical impedance spectroscopy (EIS). It was found that the API self-assembled monolayer (SAM) was formed with the concentration of 1.0 mM of API at 24 h assembling time and the maximum inhibition efficiency that could be achieved was 93.10%. The API SAM on copper was characterized by Fourier transform infrared spectroscopy (FT-IR), energy dispersive X-ray analysis (EDX), X-ray photoelectron spectroscopy (XPS), atomic force microscopy (AFM) and water contact angle measurement (WCA). The presence of N and C signals in the XPS and EDX, show that the API molecules successfully anchor on the copper surface which demonstrates formation of API SAM on the copper surface. Corrosion protection capability of the copper modified with API was evaluated by the electrochemical polarization study (EPS) and scanning electron microscopy (SEM). The results of electrochemical and SEM analysis revealed that the API modified copper showed better corrosion protection in 3% NaCl solution.

ARTICLE HISTORY
Received 6 November 2017
Accepted 19 February 2018

KEYWORDS
Copper; corrosion inhibition; self-assembled monolayer; aminopropyl imidazole; X-ray photoelectron spectroscopy

1. Introduction

Surface modification of metal surface with self-assembled monolayer (SAM) is a potent technique for the tuning and enhancement of surface properties. SAM has attracted great attention of many researchers owing to their widespread potential applications in diverse fields including molecular electronics, biosensors, corrosion protection and antimicrobial applications [1–4]. Copper (Cu) is a kind of non-ferrous metal extensively used in a wide array of applications in many fields because it possess good mechanical, thermal and electrical properties [5]. Nevertheless, one of the main disadvantages of Cu material is that it easily suffers from severe corrosion in the presence of moisture and chloride ions, especially in seawater environment. The performance of Cu is greatly affected in most of its industrial practical applications and reduces the lifespan of metals [6–10]. Alleviating the

CONTACT S. Ramesh ✉ drsramesh_56@yahoo.com

Cu corrosion in harsh corrosive environment has always been a challenging hot research topic and the study of Cu corrosion phenomena has attracted the attention of numerous investigators [11–14]. Modifications of the metal surface with self-assembled monolayer is a promising domain in protecting metals from corrosion because of their formation of compact and ordered monolayers on the substrate surface [15], which serves as a robust barrier for isolation from corrosive species and thus, reduce the speed of metal dissolution. Generally, organic inhibitors including polar functional group, π electron systems and unshared electron pairs on the hetero atom (N, S, and O) have been explored as effective corrosion inhibitors for metals in corrosive medium owing to their interaction with unoccupied d-orbitals of metals leading to the formation of an adherent protective layer on the surface which provides barrier properties for the metal substrate [16–18]. Several scientific studies have been devoted to the topic of corrosion inhibition by different types of azole inhibitors utilized for many metals and alloys in various aggressive media [13,16,19–23].

Unfortunately, many of the commonly used effective organic inhibitors are toxic for living beings and harm the environment. Thus, there is a growing concern to find safe, highly efficient, low-toxic, environment friendly film forming substances replacing harmful inhibitors for protection of Cu surface from corrosion in harsh environment. Imidazole and their derivatives have been reported as non-toxic and good corrosion inhibitors for various metals in acid solution as well as neutral media [12,24–28]. Imidazoles are organic heterocyclic compounds showing three different possible attaching modes suitable for bonding with substrate surface: pyrrole like nitrogen atom-1 N, pyridine like nitrogen atom-3 N and aromatic ring itself as well as probably the substituent may behave as an active center [12].

To the best of our knowledge, no reports are available for 1-(3-aminopropyl imidazole) (API) derivative with respect to the literature on API SAM for the protection of Cu corrosion in 3% NaCl solution (Figure 1). The present work was intended to prepare API monolayer on Cu surface via self-assembly and an attempt made to explore the anti-corrosion performance of SAM for Cu in corrosive environment. The SAM modified Cu surface was characterized by Fourier transform infrared spectroscopy (FT-IR), energy dispersive X-ray analysis (EDX), X-ray photoelectron spectroscopy (XPS), atomic force microscopy (AFM) and water contact angle measurement (WCA). Moreover, electrochemical polarization study (EPS) and scanning electron microscopy (SEM) measurements were employed to appraise the corrosion protection abilities of API for Cu in 3% NaCl solution.

2. Experiment details

2.1. Materials and sample preparation

1-(3-aminopropyl) imidazole was supplied by Sigma–Aldrich (API, 97%) while other materials used in this study, sodium chloride (NaCl) and absolute ethanol (CH_3CH_2OH) were

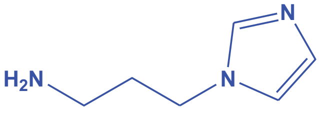

1-(3-aminopropyl)imidazole

Figure 1. Molecular structure of 1-(3-aminopropyl) imidazole.

of analytical reagent grade (AR). The API inhibitor was dissolved in absolute ethanol to prepare 0.1–1.5 mM solutions. The Cu samples of different dimensions employed for surface analytical studies (1.0 × 1.0 × 0.1 cm) and were cut from Cu sheet with 99.9% purity. For the electrochemical investigation, the working electrode of geometrical square surface of only 1 cm^2 area was exposed to the corrosive solution while the rest part was sealed in a Teflon sheath. The sample surface was ground through a series grade of emery papers of up to 6/0 grade and polished with alumina slurry (0.3 μm) and sequentially rinsed with double distilled water, then sonicated in ethanol for 10 min and finally dried with a flow of N_2 gas.

2.2. Formation of API SAM on Cu

The polished Cu samples were etched in concentrated solution of HNO_3 (7 M) for 30 s to provide a fresh and oxide-free active surface to form a high quality SAM [29,30]. The etched samples were washed with the double distilled water followed by ethanol and then the pre-treated samples were forthwith immersed in different concentrations of API solution in ethanol for different assembly times at room temperature. At the end of surface modification, the samples were taken out from the SAM solution and rinsed with ethanol followed by double distilled water to eliminate loosely bound API molecules on the electrode surface and then dried by flowing N_2 gas prior to further exploration.

2.3. Electrochemical methods

Electrochemical methods provide a powerful tool for measuring the surface characteristics of metals modified by SAMs in corrosive environment [31]. Electrochemical measurements were recorded with CHI electrochemical analyzer (CHI 760D) in a conventional three electrode cell which comprised a saturated calomel electrode (SCE) and platinum electrode serving as the reference and auxiliary electrodes, respectively. The bare Cu or API SAM modified Cu sample was adopted as the working electrode. Prior to each electrochemical test, the Cu sample was immersed in 3% NaCl medium for 1 h to reach an almost steady condition. The impedance spectroscopy measurements were performed under open circuit potential (OCP) ranging from 100 kHz to 0.1 Hz with AC signal amplitude of 5 mV. The resulting impedance results were investigated by ZSimpWin 3.2.1 software and fitted to the suitable electrical equivalent circuits. The polarization studies were recorded from –0.5 to +0.2 V with a scan rate of 2 mV s^{-1}.

2.4. Surface analytical studies

FT-IR spectra of the pure API and API SAM on Cu samples were measured with JASCO 460 plus model spectrometer. Each spectrum was recorded in a single reflection mode and its spectral range lies between 400 and 4000 cm^{-1} with 32 scans and 4 cm^{-1} resolution. The surface morphologies and elemental analysis of the Cu sample surface with and without API SAM were analyzed by SEM (VEGA3 TESCAN) attached with EDX (Bruker Nano, Germany). The contact angles of water droplets were tested on a contact angle goniometer (250-F1, rame-hart instrument Co., USA) by sessile droplet method using 10 μL water. The contact angle data were collected by measuring five different locations on every Cu sample and then averaged to obtain reliable values. The XPS studies of Cu samples in the absence and presence of SAM were recorded on a Thermo scientific X-ray photoelectron spectrometer with a monochromated Al Ka X ray source (1486.6 eV). The surface roughness and topography of the sample surfaces were examined using contact mode atomic force microscopy (BT 02218, Nanosurf, Switzerland) and scan area of 10 µm × 10 µm is evaluated for a set point of 20 nN and a scan speed of 10 mm s^{-1}.

3. Results and discussion

3.1. Electrochemical impedance studies

3.1.1. Effect of API concentration

Figure 2 shows the Nyquist plots for the bare Cu and API covered Cu electrodes after the 24 h of assembly in various concentrations of API solution. For the bare Cu sample (Figure 2(a), inset), Nyquist curve showed a depressed capacitive arc in the high frequency and followed by Warburg impedance (W) at low frequency in the real axis. The presence of W in the low frequency region represent the transport of soluble $CuCl_2^-$ products from electrode interface to the bulk solution (anodic diffusion) [32], and or the oxygen transport from the bulk solution to the surface of the Cu substrate (cathodic diffusion) [33]. For the API modified Cu electrode, the W disappeared at low frequencies, indicating that the SAM is sufficiently densely packed to prevent the diffusion process of the corrosion reaction and the Cu corrosion is controlled by the charge transfer process. The Nyquist plots show several impedance loops in the real axis in which the size of the loops were sharply enlarged by increasing the concentration of API, implying the formation of more compact and insulating film on the Cu surface. Figure 2(b) depicts the Bode plots of (phase angle vs. frequency and impedance vs. frequency) bare and API SAM modified Cu electrodes, respectively. Bode plots of (phase angle vs. frequency) modified Cu sample displays a broader shape, maximum shift in the phase angle value at high frequency area which increases with enhancing the API concentration. The increase of the phase value in the presence of the SAM shows more API molecules were adsorbed on the Cu surface at the higher concentration of API. Whereas the Bode plot of (impedance vs. frequency) exhibits that the Bode amplitude values over the entire frequency range increases with the incremental concentration of API. This result indicates the formation of denser and highly organized SAM on the electrode surface. The experimental impedance data were analyzed and best fitted by equivalent electrical circuits (EECs) (Figure 3) and their corresponding impedance parameters are summarized in Table 1. In the EECs, R_s stands for the electrolytic solution resistance, R_{ct} is the charge transfer resistance, R_{sam} the resistance of API SAM formed on the Cu surface, W represents the Warburg impedance, CPE_{dl} is the constant phase element of electrical double layer and CPE_{sam} represents the constant phase element of SAM. It can be seen that Nyquist impedance plots show imperfect capacitive arcs with its center below the real portion which can be accredited to the frequency dispersion arising from the surface roughness and non-uniformity of the substrate surface. Therefore, a constant phase element (CPE) is typically utilized in place of double layer capacitance (C_{dl}) in the electrochemical equivalent circuit to fit the depressed curve more correctly [34]. The admittance and impedance of a CPE are described by the following equation.

$$Y_{\mathrm{CPE}} = Y_0(j\omega)^n \text{ and } Z_{\mathrm{CPE}} = \frac{1}{Y_0(j\omega)^{-n}} \tag{1}$$

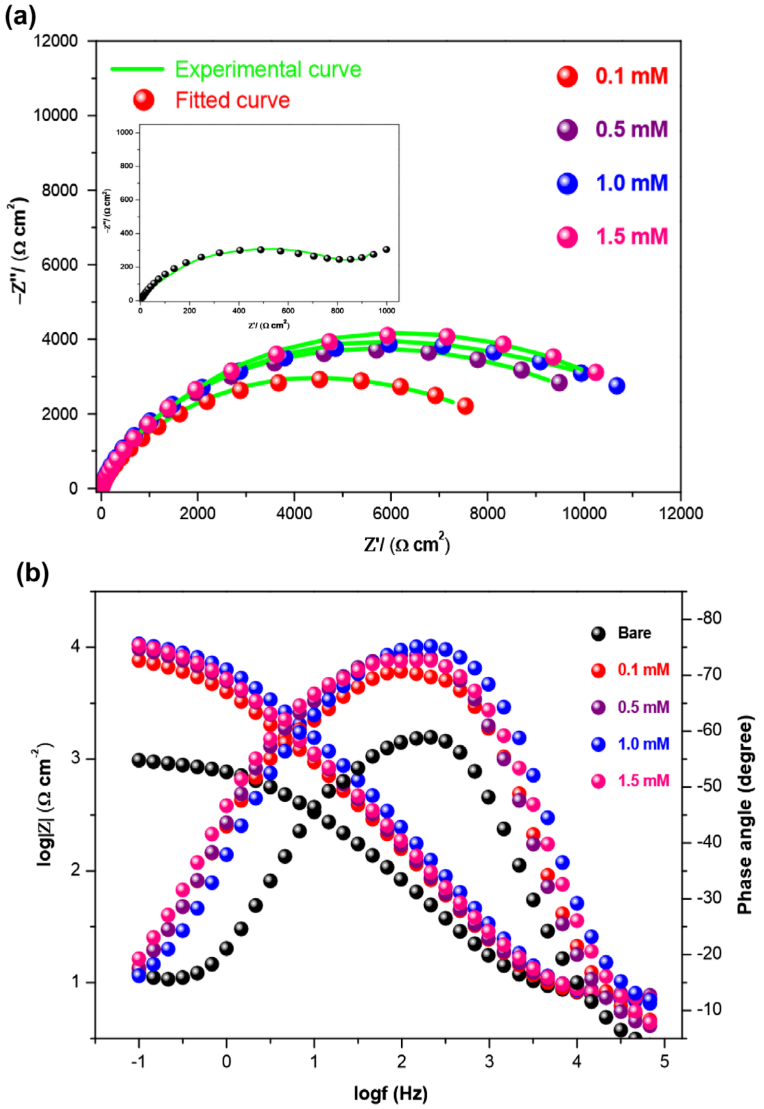

Figure 2. (a) Nyquist and (b) Bode plots obtained in 3% NaCl for bare Cu and API modified Cu electrodes assembled in different concentrations of API solution for 24 h. (inset Figure 2a: Nyquist spectra of bare Cu).

where Y_0 represents the magnitude of the CPE, j stands for the imaginary root, ω is the angular frequency and n is the exponential term of the CPE. The n value indicates the state of the Cu electrode surface. Smaller n value infers a rougher sample surface and the value of n for a real electrode often lie between 0 and 1. The inhibition efficiency (IE) is evaluated using equation [23].

$$\mathrm{IE}(\%) = \frac{R'_{ct} - R_{ct}}{R'_{ct}} \times 100 \tag{2}$$

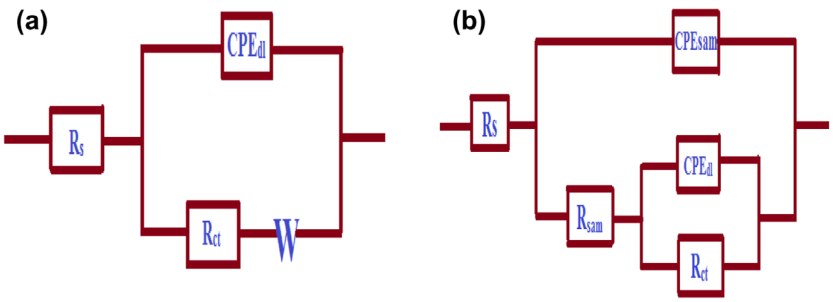

Figure 3. Equivalent circuit models of (a) bare Cu and (b) API SAM modified Cu electrodes in 3% NaCl solution.

Table 1. Nyquist impedance parameters for the bare Cu and API modified Cu electrodes assembled in different concentrations of API solution for 24 h in 3% NaCl solution.

C (mM)	R_{ct} (Ω cm^2)	CPE$_{dl}$ (μF cm^{-2})	n_1	R_{sam} (Ω cm^2)	CPE$_{sam}$ (μF cm^{-2})	n_2	χ^2	IE (%)
0	806	97.06	0.68	–	–	–	1.641×10^{-3}	–
0.1	8558	50.18	0.50	1549	25.44	0.83	7.972×10^{-3}	90.58
0.5	10,685	48.29	0.52	2564	21.34	0.87	6.699×10^{-3}	92.45
1.0	11,690	44.94	0.54	2841	13.77	0.88	7.245×10^{-3}	93.10
1.5	11,773	33.00	0.52	2007	22.14	0.86	6.948×10^{-3}	93.15

where R'_{ct} and R_{ct} are the charge transfer resistance for the API modified Cu and bare Cu, respectively. It is clear from Table 1 that compared with the bare Cu, R_{ct} values of Cu with API SAM increase greatly and the CPE values decrease. Moreover, the R_{ct} values increase and the CPE values decrease by raising the API concentration. The increase in R_{ct} value could be attributed to the formation of a barrier layer on the electrode surface that isolates the Cu from dissolution. The reduction in CPE values with an increase in the concentration of the API which is anticipated to cover the charged substrate surface and decrease the capacitive effect [35]. Additionally, inhibitor molecules provide lower CPE values which can be due to the gradual replacement of water molecules by API molecule at the sample surface. The values of n increments with increasing concentration of inhibitor, reveals that the morphology of electrode surface becoming homogenous and less rough due to strongly anchored API molecules on the most active site at the Cu surface. The change of n value may be attributed to the increase of inhibitor concentration resulted in a disparity in electrode surface roughness. It is found that as the concentration of API increases from 0.1 to 1.0 mM, the R_{ct} value increased from 8558 to 11,690 Ω cm^2. In addition, the values of IE increase with inhibitor concentration getting a maximum value (93.10%) at 1.0 mM. Further, the increase in concentration of API up to 1.5 mM, the R_{ct} and IE value increased slightly (11,773 Ω cm^2 and 93.15%). These results demonstrate that API inhibitor has a good performance of corrosion inhibition by forming densely packed monolayer on the Cu surface at the 1.0 mM concentration. Therefore, the 1.0 mM concentration of API was optimized to prepare the SAM on the Cu surface.

3.1.2. Effect of assembly time

Figure 4 presents the Nyquist and Bode plots for bare Cu and API modified Cu electrodes in 3% NaCl solution after different assembly times in the range of 1 to 30 h with the fixed

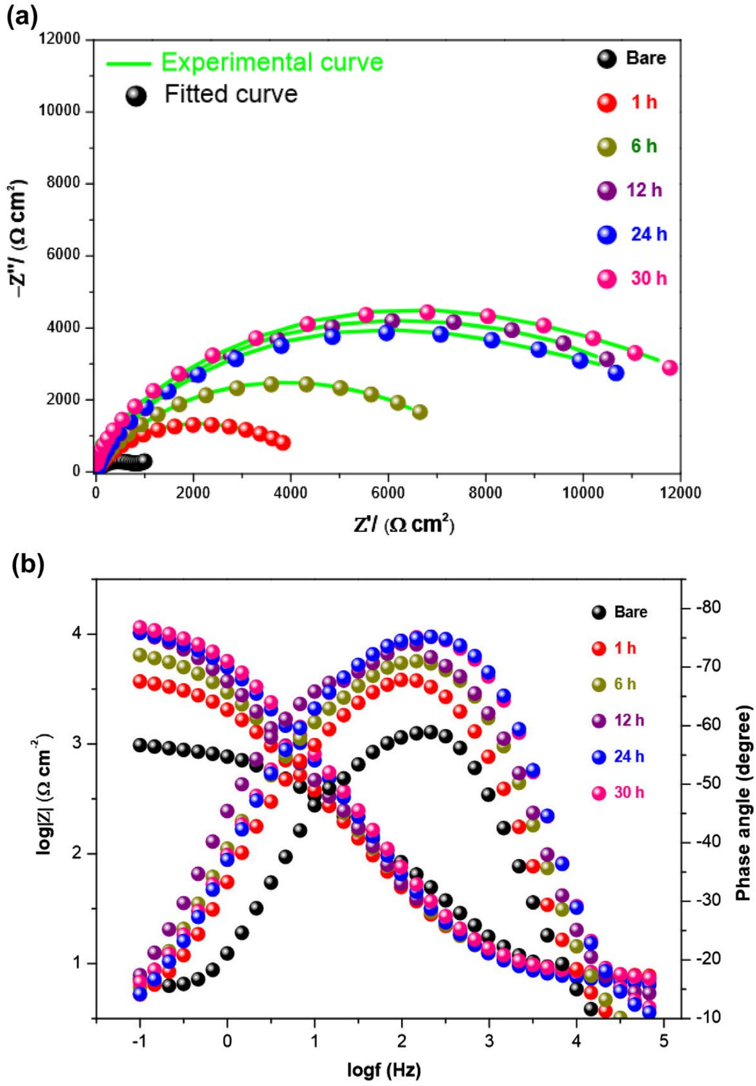

Figure 4. (a) Nyquist and (b) Bode plots obtained in 3% NaCl for bare Cu and API modified Cu electrodes assembled in 1.0 mM API solution for different times.

concentration of 1.0 mM API. The corresponding impedance parameters are summarized in Table 2. For the Cu modified by API for 1 and 6 h, the R_{ct} values are 3738 and 7081 Ω cm^2, respectively and the IE values are 78.43 and 88.61%, respectively. While the assembly time was further raised to 12 h, the value of R_{ct} reached 10,010 Ω cm^2 with an IE of 91.94%. When the assembly time increased to 24 h, the values of R_{ct} and IE reach the maximum values of 11,690 Ω cm^2, 93.10%, respectively. However, the increases R_{ct} and IE values of 30 h is relatively less R_{ct} (12,026 Ω cm^2) and IE (93.29%) values when compared to 24 h of assembly time on modified electrode. It indicates that the API molecules on Cu surface have attained a saturated state after the self-assembling time of 24 h. The above results indicate that the suitable assembly time is 24 h for the successful formation of SAM with maximum surface coverage.

Table 2. Nyquist impedance parameters for the bare Cu and API modified Cu electrodes assembled in 1.0 mM API solution for different times in 3% NaCl solution.

t (h)	R_{ct} (Ω cm^2)	CPE$_{dl}$ (μF cm^{-2})	n_1	R_{sam} (Ω cm^2)	CPE$_{sam}$ (μF cm^{-2})	n_2	χ^2	IE (%)
0	806	97.06	0.68	–	–	–	1.641×10^{-3}	–
1	3738	96.62	0.48	1055	35.95	0.83	9.103×10^{-3}	78.43
6	7081	53.11	0.51	1345	22.87	0.86	7.486×10^{-3}	88.61
12	10,010	39.65	0.53	3781	23.58	0.85	2.617×10^{-3}	91.94
24	11,690	44.94	0.54	2841	13.77	0.88	7.245×10^{-3}	93.10
30	12,026	32.57	0.50	2798	11.38	0.89	8.318×10^{-4}	93.29

From the above results it is concluded that the optimum conditions for the formation of API SAM on Cu surface are 1.0 mM concentration of API in ethanol and an assembly time of 24 h. These conditions were utilized for the formation of API SAM on Cu surface throughout the studies.

3.2. Characterization of API SAM on Cu

3.2.1. FT-IR spectroscopy

FT-IR spectroscopy studies were carried out to confirm the surface modification on the Cu surface. Figure 5 shows the FT-IR spectrum of pure API and API SAM formed on the Cu substrate, respectively. The bands were assigned to the pure API as follows (Figure 5(a)): the bands at 1572 cm^{-1} (C=N stretching), 1392 cm^{-1} (C–N stretching) and 3424 cm^{-1} (N–H stretching) [36]. On the other hand, API modified Cu showed some main bands that are characteristically different than observed for pure API. The spectrum of API with Cu (Figure

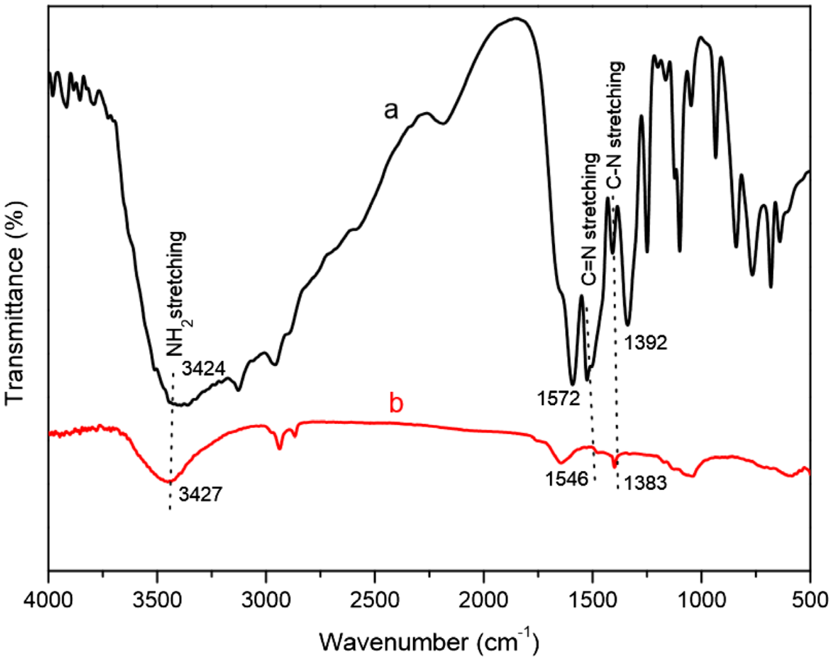

Figure 5. FT-IR spectra of (a) pure API and (b) API SAM formed on Cu.

5(b)) showed the shifting of characteristic C=N stretching band from 1572 to 1546 cm^{-1} and C–N stretching band shifting from 1392 to 1383 cm^{-1}. From the above observations, it can be concluded that there is successful formation of the API SAM on the Cu by the N atom of imidazole ring.

3.2.2. SEM and EDX analysis

The surface morphology and elemental composition of polished Cu and API SAM modified Cu surfaces were measured by SEM and EDX techniques (Figure 6). Figure 6(a) illustrates the SEM image of polished Cu surface which appeared uniform with scratches and some nicks spread over its surface. This could be due to surface pretreatment with different grades of emery papers and retains the polished sample surface. The corresponding EDX spectrum showed the elemental signal for Cu (89.48 at.%) at 0.93 and 8.05 keV, and O (10.52 at.%) at 0.53 keV, respectively (Figure 6(b)). On the other hand, API modified Cu (Figure 6(c)) seemed a smooth surface with dense organic layer, indicating the successful assembly of API SAM over Cu surface. This results was further evidenced by EDX which showed four elemental peaks at C (27.90 at.%) at 0.28 keV, N (4.78 at.%) at 0.39 keV, O (1.76 at.%) at 0.53 keV and Cu (65.76 at.%) at 0.93 and 8.05 keV for API modified Cu (Figure 6(d)). The

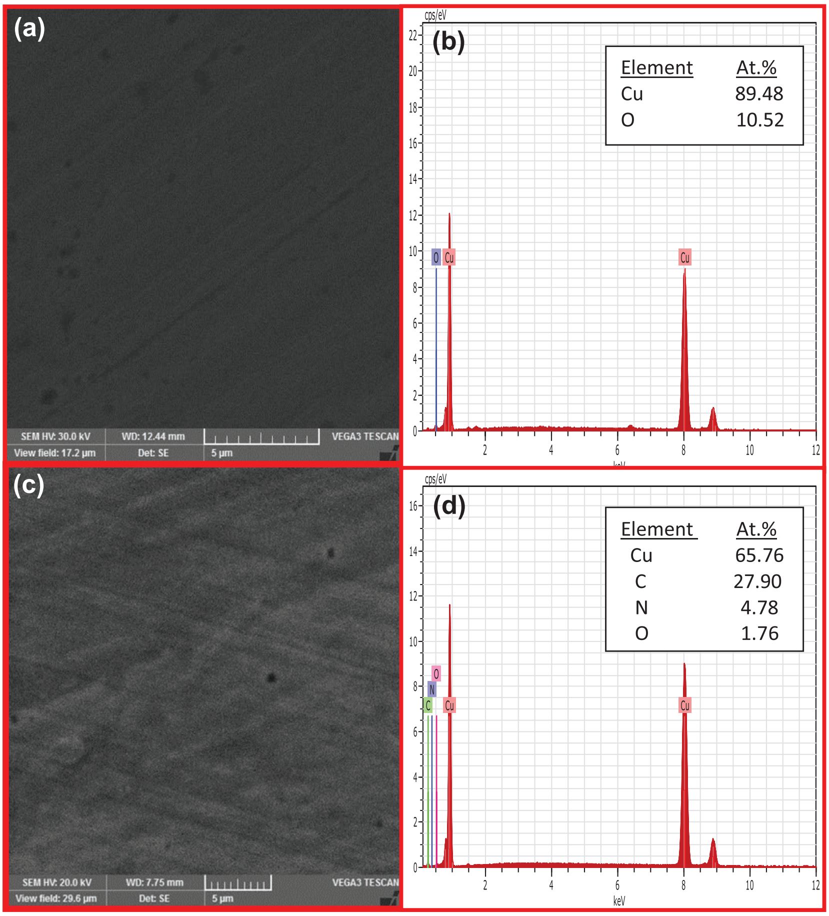

Figure 6. SEM images and EDX spectra of polished Cu (a, b) and API SAM modified Cu (c, d).

detection of C and N signals at 0.28 and 0.39 keV on the surface confirmed the API SAM formation on the Cu surface.

3.2.3. XPS analysis

In order to further corroborate the surface modification and the chemical state on the Cu surface they were studied by XPS for both polished Cu and API SAM modified samples. Wide scan and deconvolutated XPS spectra of the polished Cu sample are depicted in Figure 7. Figure 7(a) shows the wide scan spectrum of polished Cu. The XPS Cu 2p spectrum of Figure 7(b), showed two signals at 932.6 and 952.4 eV that are assigned to binding energy of Cu $2p_{3/2}$ and Cu $2p_{1/2}$, respectively, implying the presence of Cu (I) [13]. The O 1s signal (Figure 7(c)) at 531.5 eV is ascribed to the formation of Cu_2O on the Cu surface [37]. Further, the wide scan and deconvolutated XPS spectra of the API SAM modified Cu sample are shown in Figure 8. Wide scan spectrum of API modified Cu displayed in Figure 8(a). In Figure 8(b), the Cu 2p spectra exhibit two signals at 932.7 and 952.5 eV, respectively.

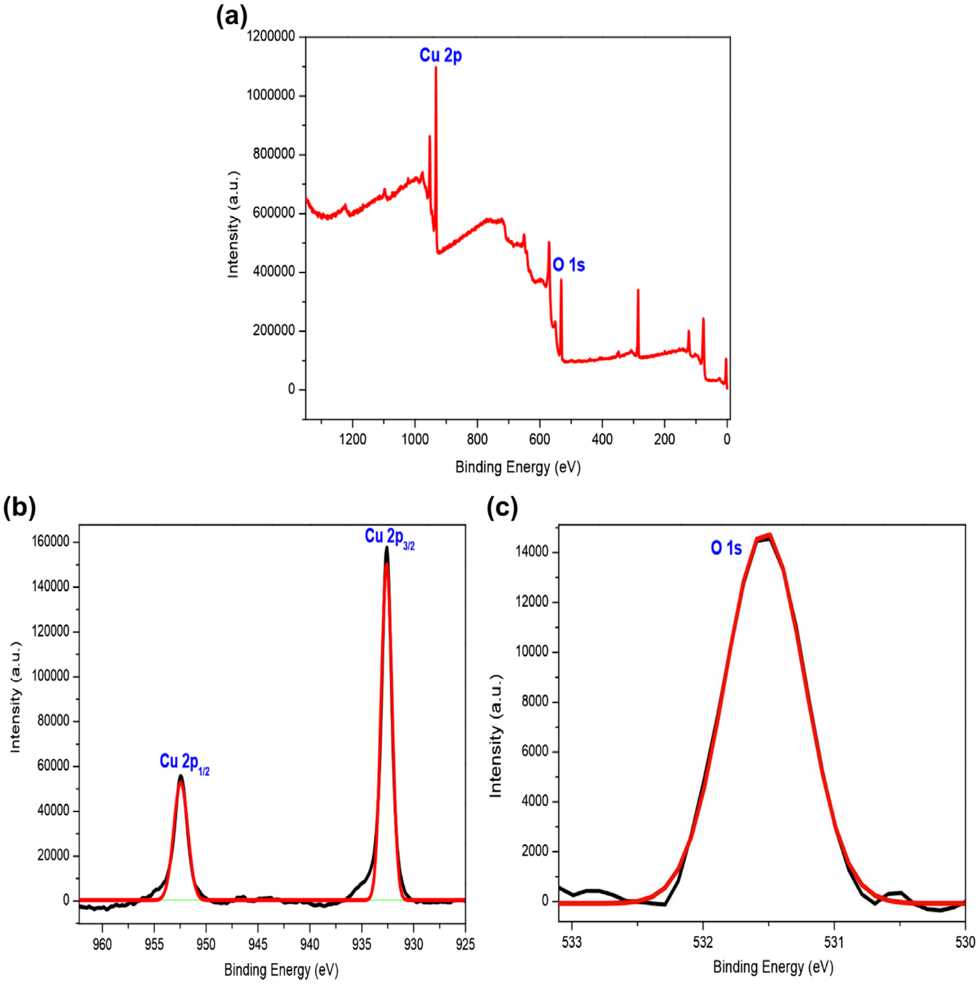

Figure 7. XPS of wide scan (a) and deconvoluated spectra of (b) Cu 2p (c) O 1s of polished Cu.

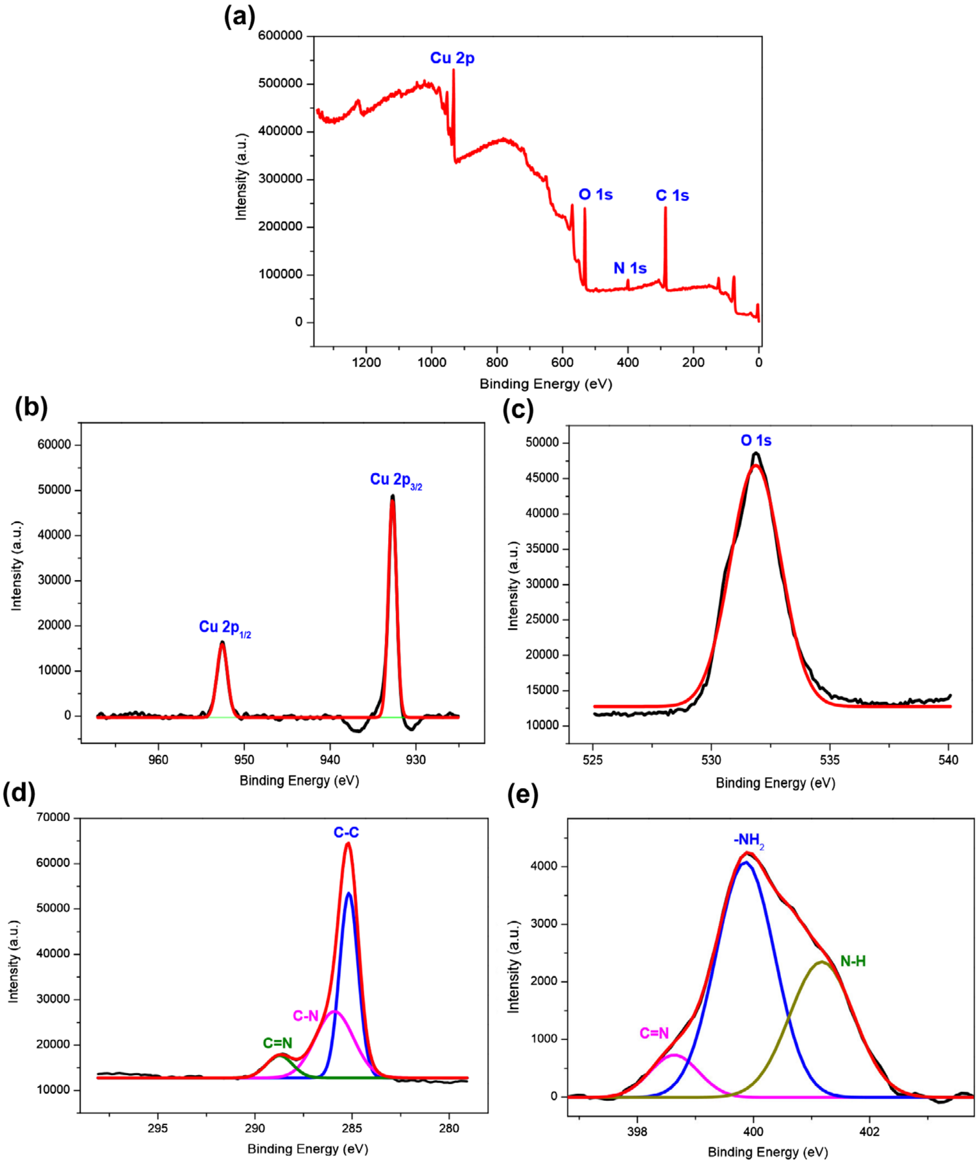

Figure 8. XPS of wide scan (a) and deconvoluated spectra of (b) Cu 2p (c) O 1s (d) C 1s and (e) N 1s of API SAM modified Cu.

The signal at higher binding energy can be accredited to Cu $2p_{1/2}$ and the signal at lower binding energy can be ascribed to Cu $2p_{3/2}$ which is due to initial oxidation of Cu to Cu_2O during SAM formation. The signal at 531.7 eV in O 1s spectrum (Figure 8(c)) can be attributed to the Cu_2O. The presence of oxygen in the SAM Cu showed that oxygen dissolved in the API solution participates in the self-assembly process. The absence of satellite signals around the binding energy of 943–963 eV suggested that there is no Cu (II) formed on the surface. The spectrum of C 1s of the API modified Cu surface consist of three signals with the characteristic binding energy at 284.1, 285.9 and 288.7 eV associated with the C–H, C–N and C=N, respectively (Figure 8(d)). The N 1s displayed three signals (Figure 8(e)). The dominant signal at binding energy of 399.9 eV is ascribed to the terminal $-NH_2$, and the other signals at binding energy of 398.7 and 401.2 eV were attributed to the C=N and N–H in the imidazole ring, respectively [38]. The characteristic binding energy of the elemental nitrogen and free amine signals were reported at 398.0 eV [39], and 400.1 eV [40], respectively. The shift of N 1s binding energy (398.7 eV) from elemental binding energy (398.0 eV) showed that the API molecule is chemically absorbed on Cu surface via the N atoms of imidazole ring.

3.2.4. AFM analysis

The surface topography of the Cu samples with and without API SAM were examined by AFM. The AFM pattern of the 2D, 3D-Topography of the polished Cu and API modified Cu samples are shown in Figure 9. Average surface roughness (S_a) and root mean square (S_q) values for polished Cu and modified Cu were obtained from respective AFM images. Figure 9(a) showed that the polished surface was flat with some tiny polishing scratches on the surface with S_a and S_q values of 19.766 and 24.965 nm, respectively. Whereas, the modified surface (Figure 9(b)) was having a comparatively uniform surface morphology with S_a and S_q values of 15.735 and 19.713 nm, respectively. After modification with SAM,

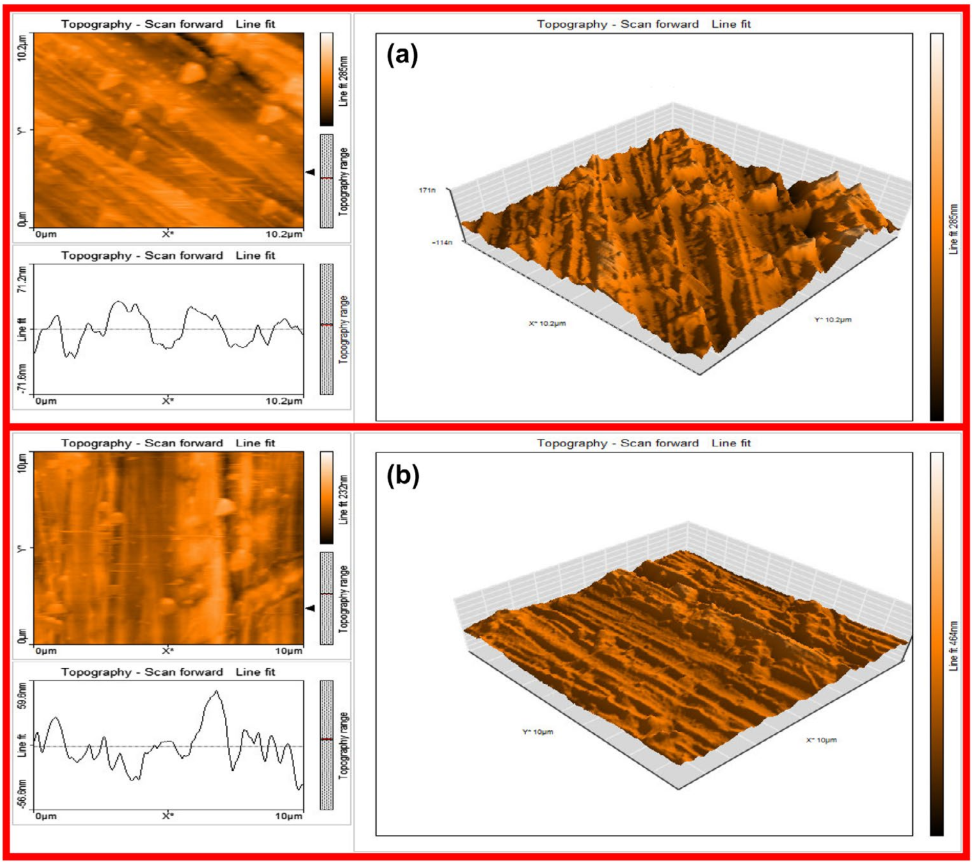

Figure 9. AFM patterns of (a) polished Cu and (b) API SAM modified Cu.

significant reduction in S_a and S_q values were observed when compared to that of polished sample which clearly point out the surface modification on the Cu surface.

3.2.5. WCA analysis

WCA measurements were performed to assess the surface wetting behavior of the Cu surface before and after modification. The photographic images of the sessile water drop on polished Cu and API modified Cu substrate surfaces are shown in Figure 10. For the polished Cu (Figure 10(a)), the WCA value is about 77.5° while for the Cu sample covered by API monolayer, the WCA value increased to 91.8° (Figure 10(b)). The significant increases of WCA value indicate that the SAM molecules have been successfully self-assembled on the Cu surface.

3.3. Assessment of corrosion protection of Cu by API SAM

3.3.1. Electrochemical polarization studies

Figure 11 presents the electrochemical polarization curves of the bare Cu and the API modified Cu electrodes in 3% NaCl solution. The electrochemical kinetic corrosion parameters of Cu without and with SAM were derived from the Tafel curves as corrosion potential (E_{corr}), corrosion current density (i_{corr}), anodic Tafel slope (b_a), cathodic Tafel slope (b_c) and IE are given in Table 3. The percentage of IE can be evaluated as follows

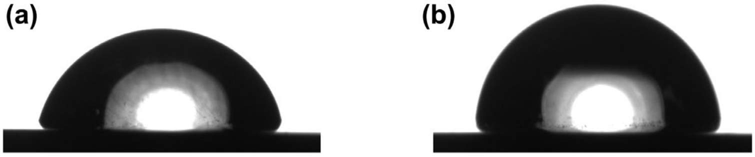

Figure 10. Contact angle images of (a) polished Cu and (b) API SAM modified Cu.

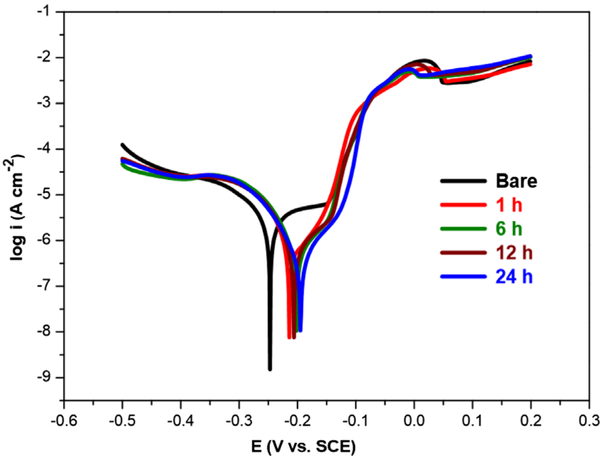

Figure 11. Electrochemical polarization curves obtained in 3% NaCl solution for bare Cu and API modified Cu assembled in 1.0 mM API solution for different times.

Table 3. Electrochemical polarization parameters for the bare Cu and API modified Cu electrodes assembled in 1.0 mM API solution for different times in 3% NaCl solution.

t (h)	E_{corr} (mV/SCE)	I_{corr} (µA cm^{-2})	b_a (mV dec^{-1})	b_c (mV dec^{-1})	IE (%)
0	247	4.524	90	201	–
1	214	0.626	24	173	86.16
6	202	0.527	25	142	88.35
12	206	0.489	23	153	89.19
24	195	0.259	19	104	94.27

$$\mathrm{IE}(\%) = \frac{i^0_{\mathrm{corr}} - i_{\mathrm{corr}}}{i^0_{\mathrm{corr}}} \times 100 \tag{3}$$

where i^0_{corr} and i_{corr} are the corrosion current densities of the bare and API SAM modified Cu, respectively. It is clear from Figure 11, as compared with the bare Cu, the anodic and cathodic polarization curves of the API modified Cu move towards lower current densities along with the E_{corr} which shifted towards more positive direction. Moreover, E_{corr} shift was only slight with the increment of assembly time, suggesting that the API mainly impedes the dissolution rate of Cu in NaCl solution. For the bare Cu, i_{corr} value is 4.524 µA cm^{-2}, whereas for the Cu modified with API SAM, the value of i_{corr} decreased from 0.626 to 0.259 µA cm^{-2}. The decrease in the i_{corr} value is mainly due to the lack of interaction of Cl$^-$ on the Cu surface. Therefore, it has improved anticorrosion properties for Cu surface after the modification by API SAM. It is seen that the IE increased with increasing of assembly time and the corrosion protection efficiency reached a maximal value of 94.27%. In comparison with the bare Cu, the E_{corr} of the SAM Cu moves towards the positive region and all the displacements were lower than 85 mV/SCE suggesting a mixed type corrosion inhibitor [41], predominantly inhibiting the anodic reaction. The positive shift of the E_{corr}

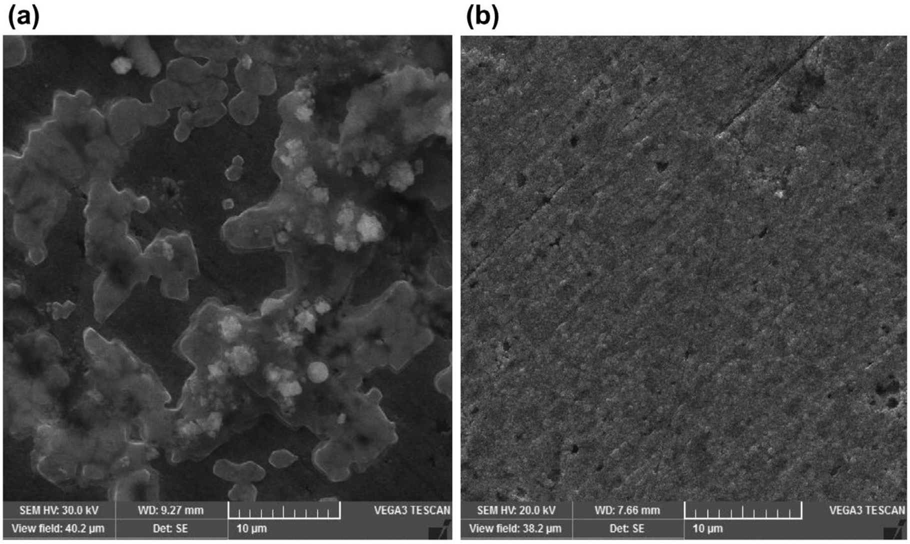

Figure 12. SEM images of (a) bare Cu and (b) API SAM modified Cu after immersed in 3% NaCl solution for 72 h.

and reduction of the I_{corr} revealed that the presence of API SAM has greatly improved the corrosion resistance for Cu in NaCl solution.

3.3.2. SEM studies

The surface morphologies of the bare Cu and Cu surface covered by API SAM after 72 h exposure in aqueous 3% NaCl environment was studied by SEM and are represented in Figure 12. In Figure 12(a), bare Cu surface in NaCl solution was severely deteriorated and the rough surface is due to the Cu dissolution in the corrosive environment. Compared with the bare sample, the morphology of surface was distinctly different for the API SAM modified Cu after immersion in corrosive environment. As it can be seen from Figure 12(b), the surface relatively looked to be of much less corroded morphology which reveals that the formed API SAM effectively protects the Cu in 3% NaCl solution.

4. Conclusion

We have successfully prepared API SAM on a Cu surface by self-assembly technique. API SAM was characterized by FT-IR, SEM-EDX, WCA, AFM and XPS analysis. EIS results indicate that the R_{ct} of the Cu with API increase markedly and its CPE values decrease significantly. Electrochemical polarization plots show that the API behaves as mixed type inhibitor, predominantly anodic in nature with IE value of 94.27%. The SEM analysis showed that the formed API SAM on Cu increased the anticorrosion properties of Cu.

Acknowledgments

P. Durainatarajan is grateful to the UGC-RFSMS (Research Fellowship in Sciences for Meritorious Students, Grant No: F.No.25-1/2014-15/(BSR)/7-225/2008/(BSR), dt: 7th October 2015) for financial support and also the authorities of The Gandhigram Rural Institute – Deemed to be University for encouragement.

Disclosure statement

No potential conflict of interest was reported by the authors.

Funding

P. Durainatarajan is financially supported by the UGC-RFSMS (Research Fellowship in Sciences for Meritorious Students [grant number F.No.25-1/2014-15/(BSR)/7-225/2008/(BSR)], dt: 7th October 2015).

References

[1] Love JC, Estroff LA, Kriebel JK, et al. Self-assembled monolayers of thiolates on metals as a form of nanotechnology. Chem Rev. 2005;105:1103–1170.
[2] Nelson B, Schwartz DT. Electrochemical factors controlling the patterning of metals on SAM-coated substrates. Langmuir. 2007;23:9661–9666.
[3] Hukovi MM, Babic R, Petrovi Z, et al. Copper protection by a self-assembled monolayer of alkanethiol comparison with benzotriazole. J Electrochem Soc. 2007;154:C138–C143.

[4] Jon S, Seong J, Khademhosseini A, et al. Construction of nonbiofouling surfaces by polymeric self-assembled monolayers. Langmuir. 2003;19:9989–9993.

[5] Scendo M. The effect of purine on the corrosion of copper in chloride solutions. Corros Sci. 2007;49:373–390.

[6] Laibinis PE, Whitesides GM. Self-assembled monolayers of n-alkanethiolates on copper are barrier films that protect the metal against oxidation by air. J Am Chem Soc. 1992;114:9022–9028.

[7] Núñez L, Reguera E, Corvo F, et al. Corrosion of copper in seawater and its aerosols in a tropical island. Corros Sci. 2005;47:461–484.

[8] Liang C, Wang P, Wu B, et al. Inhibition of copper corrosion by self-assembled monolayers of triazole derivative in chloride-containing solution. J Solid State Electrochem. 2010;14:1391–1399.

[9] El Warraky A, El Shayeb HA, Sherif EM. Pitting corrosion of copper in chloride solutions. Anti-Corros Meth Mater. 2004;51:52–61.

[10] Kear G, Barker BD, Walsh FC. Electrochemical corrosion of unalloyed copper in chloride media – a critical review. Corros Sci. 2004;46:109–135.

[11] Shaban A, Kálmán E, Telegdi J, et al. Corrosion and inhibition of copper in different electrolyte solutions. Appl Phys A. 1998;66:S545–S549.

[12] Zhang Z, Chen S, Li Y, et al. A study of the inhibition of iron corrosion by imidazole and its derivatives self-assembled films. Corros. Sci. 2009;51:291–300.

[13] Wang CT, Chen SH, Ma HY, et al. Study of the stability of self-assembled N-vinylcarbazole monolayers to protect copper against corrosion. J Serb Chem Soc. 2002;67:685–696.

[14] Chen W, Hong S, Li HB, et al. Protection of copper corrosion in 0.5 M NaCl solution by modification of 5-mercapto-3-phenyl-1,3,4-thiadiazole-2-thione potassium self-assembled monolayer. Corros Sci. 2012;61:53–62.

[15] Ulman A. Formation and structure of self-assembled monolayers. Chem Rev. 1996;96:1533–1554.

[16] Antonijević MM, Milić SM, Petrović MB. Films formed on copper surface in chloride media in the presence of azoles. Corros Sci. 2009;51:1228–1237.

[17] Sherif EM, Almajid A. Surface protection of copper in aerated 3.5% sodium chloride solutions by 3-amino-5-mercapto-1, 2, 4-triazole as a copper corrosion inhibitor. J Appl Electrochem. 2010;40:1555–1562.

[18] Qiang Y, Zhang S, Xu S, et al. The effect of 5-nitroindazole as an inhibitor for the corrosion of copper in a 3.0% NaCl solution. RSC Adv. 2015; 5: 63866–63873.

[19] Subramanian R, Lakshminarayanan V. Effect of adsorption of some azoles on copper passivation in alkaline medium. Corros Sci. 2002;44:535–554.

[20] Li WH, He Q, Pei CL, et al. Experimental and theoretical investigation of the adsorption behaviour of new triazole derivatives as inhibitors for mild steel corrosion in acid media. Electrochim Acta. 2007;52:6386–6394.

[21] Es-Salah K, Keddam M, Rahmouni K, et al. Aminotriazole as corrosion inhibitor of Cu–30Ni alloy in 3% NaCl in presence of ammoniac. Electrochim Acta. 2004;49:2771–2778.

[22] Döner A, Solmaz R, Özcan M, et al. Experimental and theoretical studies of thiazoles as corrosion inhibitors for mild steel in sulphuric acid solution. Corros Sci. 2011;53:2902–2913.

[23] Appa Rao BV, Narsihma Reddy M. Formation, characterization and corrosion protection efficiency of self-assembled 1-octadecyl-1H-imidazole films on copper for corrosion protection. Arab J Chem. 2017;10:S3270–S3283.

[24] Dafali A, Hammouti B, Aouniti A, et al. 2-Mercapto-1-methylimidazole as corrosion inhibitor of copper in aerated 3% NaCl solution Ann. Annal Chim Sci Matér. 2000;25:437–446.

[25] Otmačić H, Stupnišek-Lisac E. Copper corrosion inhibitors in near neutral media. Electrochim Acta. 2003;48:985–991.

[26] Stupnišek-Lisac E, Gazivoda A, Madžarac M. Evaluation of non-toxic corrosion inhibitors for copper in sulphuric acid. Electrochim Acta. 2002;47:4189–4194.

[27] Appa Rao BV, Yakub Iqbal Md, Sreedhar B. Electrochemical and surface analytical studies of the self-assembled monolayer of 5-methoxy-2-(octadecylthio)benzimidazole in corrosion protection of copper. Electrochim Acta. 2010;55:620–631.

[28] Bereket G, Öğretir C, Yurt A. Quantum mechanical calculations on some 4-methyl-5-substituted imidazole derivatives as acidic corrosion inhibitor for zinc. J Mol Struct. 2001;571:139–145.

[29] Quan Z, Chen S, Cui X, et al. Factors affecting the quality and corrosion inhibition ability of self-assembled monolayers of a Schiff base. Corrosion. 2002;58:248–256.

[30] Liu T, Yin Y, Chen S, et al. Super-hydrophobic surfaces improve corrosion resistance of copper in seawater. Electrochim Acta. 2007;52:3709–3713.

[31] Ma HY, Yang C, Yin BS, et al. Electrochemical characterization of copper surface modified by n-alkanethiols in chloride-containing solutions. Appl Surf Sci. 2003;218:144–154.

[32] Li SL, Wang YG, Chen SH, et al. Some aspects of quantum chemical calculations for the study of Schiff base corrosion inhibitors on copper in NaCl solutions. Corros Sci. 1999;41:1769–1782.

[33] Feng Y, Siow KS, Teo WK, et al. Corrosion mechanisms and products of copper in aqueous solutions at various pH values. Corrosion. 1997;53:389–398.

[34] Wu X, Ma H, Chen S, et al. General equivalent circuits for faradaic electrode processes under electrochemical reaction control. J Electrochem Soc. 1999;146:1847–1853.

[35] Hong S, Chen W, Luo HQ, et al. Inhibition effect of 4-amino-antipyrine on the corrosion of copper in 3wt.% NaCl solution. Corros Sci. 2012;57:270–278.

[36] Lalitha A, Ramesh S, Rajeswari S. Surface protection of copper in acid medium by azoles and surfactants. Electrochim Acta. 2005;51:47–55.

[37] Ye XR, Xin XQ, Zhu JJ, et al. Coordination compound films of 1-phenyl-5-mercaptotetrazole on copper surface. Appl Surf Sci. 1998;135:307–317.

[38] Liu X, Chen S, Tian F, et al. Studies of protection of iron corrosion by rosin imidazoline self-assembled monolayers. Surf Interface Anal. 2007;39:317–323.

[39] Beccaria AM, Bertolotto C. Inhibitory action of 3-trimethoxysilylpropanethiol-1 on copper corrosion in NaCl solutions. Electrochim Acta. 1997;42:1361–1371.

[40] Kowalczyk D, Slomkowski S, Chehimi MM, et al. Adsorption of aminopropyltriethoxy silane on quartz: an XPS and contact angle measurements study. Int J Adhes Adhes. 1996;16:227–232.

[41] Li W, He Q, Zhang S, et al. Some new triazole derivatives as inhibitors for mild steel corrosion in acidic medium. J Appl Electrochem. 2007;38:289–295.